Perfect Recovery and Sensitivity Analysis of Time Encoded Bandlimited Signals

Aurel A. Lazar, *Fellow, IEEE,* and László T. Tóth

Abstract—A time encoding machine is a real-time asynchronous mechanism for encoding amplitude information into a time sequence. We investigate the operating characteristics of a machine consisting of a feedback loop containing an adder, a linear filter, and a noninverting Schmitt trigger. We show that the amplitude information of a bandlimited signal can be perfectly recovered if the difference between any two consecutive values of the time sequence is bounded by the inverse of the Nyquist rate. We also show how to build a nonlinear inverse time decoding machine (TDM) that perfectly recovers the amplitude information from the time sequence. We demonstrate the close relationship between the recovery algorithms for time encoding and irregular sampling. We also show the close relationship between time encoding and a number of nonlinear modulation schemes including FM and asynchronous sigma–delta modulation. We analyze the sensitivity of the time encoding recovery algorithm and demonstrate how to construct a TDM that perfectly recovers the amplitude information from the time sequence and is trigger parameter insensitive. We derive bounds on the error in signal recovery introduced by the quantization of the time sequence. We compare these with the recovery error introduced by the quantization of the amplitude of the bandlimited signal when irregular sampling is employed. Under Nyquist-type rate conditions, quantization of a bandlimited signal in the time and amplitude domains are shown to be largely equivalent methods of information representation.

Index Terms—Bandlimited signals, quantization, sampling methods, sensitivity, signal representation.

I. INTRODUCTION

A FUNDAMENTAL question arising in information processing is how to represent a signal as a discrete sequence. The classical sampling theorem ([9], [18]) calls for representing a bandlimited signal based on its samples taken at or above the Nyquist rate.

A time encoding of a bandlimited function $x(t), t \in \mathbb{R}$, is a representation of $x(t)$ as a sequence of strictly increasing times $(t_k), k \in \mathbb{Z}$, where $\mathbb{R}$ and $\mathbb{Z}$ denote the set of real numbers and integers, respectively (see Fig. 1). Alternatively, the output of the encoder is a digital signal $z(t)$ that switches between two values $\pm b$ at times $t_k, k \in \mathbb{Z}$. Time encoding is an alternative to classical sampling and applications abound. In the field of neuroscience, the representation of sensory information as a sequence of action potentials can be modeled as temporal encoding. The existence of a such a code was already postulated in [1]. Time encoding is
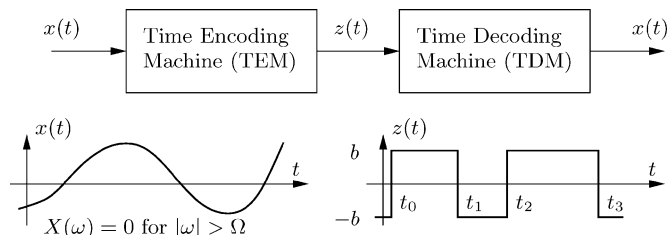
Fig. 1. Time encoding and decoding.

also of great interest for the design and implementation of future analog to digital converters. Due to the ever-decreasing size of integrated circuits and the attendant low-voltage, high-precision quantizers are more and more difficult to implement. These circuits provide increasing timing resolution, however, that a temporal code can take advantage of [16].

There are two natural requirements that a time-encoding mechanism has to satisfy [10]. The first is that the encoding should be implemented as a *real-time asynchronous* circuit. Second, the encoding mechanism should be *invertible*, that is, the amplitude information can be recovered from the time sequence with arbitrary accuracy.

The encoding mechanism investigated here satisfies both of these conditions. We show that a time encoding machine (TEM) consisting of a feedback loop that contains an adder, a linear filter and a noninverting Schmitt trigger has the required properties. We show that the amplitude information of a bandlimited signal can be *perfectly* recovered if the difference between any two consecutive values of the time sequence is bounded by the inverse of the Nyquist rate. We also show how to build a nonlinear inverse time decoding machine (TDM) (see Fig. 1) that perfectly recovers the amplitude information from the time sequence. The relationship between the recovery algorithms for time encoding and irregular sampling is described in the language of adjoint operators. We also show the close relationship between time encoding and a number of nonlinear modulation schemes including FM and Asynchronous Sigma-Delta Modulation.

The TEM considered in this paper is implemented as a nonlinear circuit. The classical Fourier analysis applied to such a circuit, has unfortunately, limited utility. An investigation of an example TEM solely based on Fourier analysis is described in [16]. Clearly, this analysis does not provide the insights and understanding needed for inverting nonlinear circuits.

The mathematical methodology used here is based on non-harmonic analysis [4], [20]. For readers who are unfamiliar with this methodology, we introduce all the concepts needed in the presentation. The time investment in this methodology turns out to be worthwhile. We demonstrate that time encoding provides

a representation modality that is on par with the classical sampling representation. However, time encoding brings an additional benefit because it is clock free. In addition, it is amenable to nano-scale implementation. This paper develops the theory of time encoding and decoding and shows the relationship to other nonlinear modulation schemes.

In practice, the question of *sensitivity* of the recovery algorithm with respect to parameter variation of the TEM is of utmost importance. In this paper, we investigate the sensitivity of signal recovery with respect to the Schmitt trigger parameter δ as well as with respect to the number N of bits used to quantize the values of the trigger times.

Through behavioral simulations, we demonstrate that the TDM that implements the perfect recovery algorithm is highly sensitive to a broad range of values of δ. Based on the simple compensation principle of [10] we provide a perfect recovery algorithm that is δ-insensitive.

We evaluate the error introduced by the quantization of the time sequence and derive bounds on the recovery error. We compare these with the recovery error introduced by the quantization of the amplitude of an arbitrary bandlimited signal when irregular sampling is employed [5]. Under Nyquist-type rate conditions, quantization of a bandlimited signal in the time and amplitude domains are shown to be largely equivalent methods of information representation. An *empirical result* describing the mean-square error (MSE) as a function of oversampling ratio σ and the number of bits N used in the representation of the time sequence is also given.

This paper is organized as follows. In Section II, a method of mapping amplitude information into a time sequence is presented. An example of a TEM is given and its stability analyzed. In order to simplify the analysis, an equivalent circuit that describes the key elements of the TEM is introduced. This circuit is used throughout the rest of the paper. Section III derives the perfect recovery algorithm. Section IV presents the relationship between irregular sampling and time encoding. The relationship to a number of nonlinear modulation schemes is also demonstrated. Section V investigates the sensitivity of the recovery algorithm with respect to the Schmitt trigger parameter δ. The compensation principle is used to build a δ-insensitive recovery algorithm. The effect of quantization of the trigger times on signal recovery is discussed in Section VI. In Section VII, the effects of quantization in the time and amplitude domains on the recovery of bandlimited signals are compared. Conclusions are drawn and future research directions are mentioned in Section VIII.

II. TIME ENCODING

The TEM investigated in this paper is depicted in Fig. 2. The filter is assumed to be an integrator. Clearly the amplitude information at the input of the TEM is represented as a time sequence at its output.

The basic principle of operation of the TEM is very simple. The bounded input signal $x(t)$, $|x(t)| \leq c < b$, is biased by a constant amount $+(-)b$ before being applied to the integrator. This bias guarantees that the integrator's output $y(t)$ is a positive (negative) increasing (decreasing) function of time. In steady
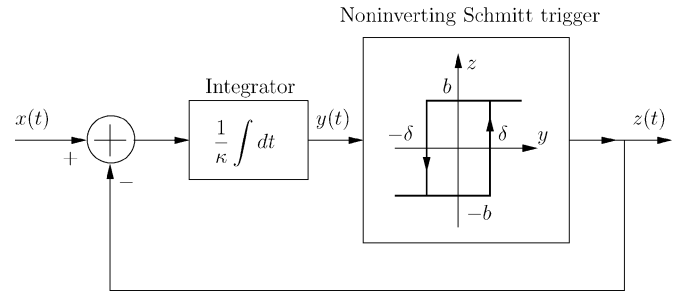

Fig. 2. Example of TEM.

state, there are two possible operating modes. In the first mode, the output of the TEM is in state $z(t) = -b$ and the input to the Schmitt trigger grows from $-\delta$ to δ. When the output of the integrator reaches the maximum value δ, a transition of the output $z(t)$ from $-b$ to $+b$ is triggered and the feedback becomes negative. In the second mode of operation, the TEM is in state $z(t) = b$ and the integrator output steadily decreases from δ to $-\delta$. When the maximum negative value $-\delta$ is reached $z(t)$ will reverse to $-b$. Thus, while the transition times of the output $z(t)$ are nonuniformly spaced, the amplitude of the output signal remains constant. Therefore, a transition of the output from $-b$ to b or vice-versa takes place every time the integrator output reaches the triggering mark δ or $-\delta$ (called quanta). The time when this quanta is achieved depends on the signal as well as on the design parameters κ, δ and b. Hence, the TEM maps amplitude information into timing information. It achieves this by a *signal-dependent* sampling mechanism.

In Sections III and IV, we discuss the conditions for stability of the TEM and introduce an equivalent circuit that describes its key elements.

A. Stability

In Fig. 2, κ, δ, and b are strictly positive real numbers and $x = x(t)$ is a Lebesgues measurable function modeling the input signal to the TEM for all t, $t \in \mathbb{R}$. The output of the integrator in a small neighborhood of t_0, $t > t_0$ is given by

$$y(t) = y(t_0) + \frac{1}{\kappa} \int_{t_0}^{t} [x(u) - z(u)]du.$$

Note that $y = y(t)$ is a continous increasing (decreasing) function whenever the value of the feedback is positive (negative). Here, $z : \mathbb{R} \rightarrow \{-b, b\}$ for all $t, t \in \mathbb{R}$, is the function corresponding to the output of the TEM in Fig. 2. z switches between two values $+b$ and $-b$ at a set of trigger times (t_k), for all k, $k \in \mathbb{Z}$, and $z(t_0) = -b$ by convention.

Remark 1: Informally, the information of the input $x(t)$ is carried by the signal amplitude whereas the information of the output signal $z(t)$ is carried by the trigger times. A fundamental question, therefore, is whether the TEM encodes information loss-free. Loss-free encoding means that the input x can be perfectly recovered from the output z.

In what follows, $1_{[t_k, t_{k+1})}(t), t \in \mathbb{R}$, denotes a pulse of length $t_{k+1} - t_k$ and unit amplitude.

Lemma 1 (Stability): For all input signals $x = x(t)$, $t \in \mathbb{R}$, with $|x(t)| \leq c < b$ the TEM is stable, i.e., $|y(t)| \leq \delta$, for all t, $t \in \mathbb{R}$. The output z is given by $z(t) =$
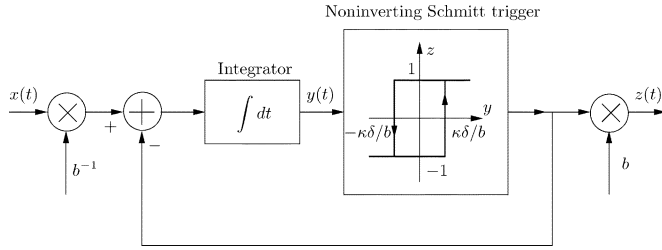
Fig. 3.   Equivalent circuit representation of the TEM.

$(-1)^{k+1}\, b\, 1_{[t_k, t_{k+1})}(t), t \in \mathbb{R}$, where the set of trigger times $(t_k), k \in \mathbb{Z}$, is generated by the recursive equation

$$\int_{t_k}^{t_{k+1}} x(u)du = (-1)^k[-b(t_{k+1} - t_k) + 2\kappa\delta] \qquad (1)$$

for all $k,\ k \in \mathbb{Z}$.

Proof: Due to the operating characteristic of the Schmitt trigger, y increases monotonically until it reaches the value δ if the feedback is b or decreases monotonically to $-\delta$ if the feedback is $-b$ for any arbitrary initial value of the integrator. After y reaches the value δ from below or $-\delta$ from above, the output of the Schmitt trigger z flips from $-b$ to b and from b to $-b$, respectively. Therefore, without loss of generality we can assume that for some initial condition at $t = t_0$ we have $(y, z) = (-\delta, -b)$ and the TEM is described in a small neighborhood of t_0, $t > t_0$, by

$$-\delta + \frac{1}{\kappa}\int_{t_0}^{t}[x(u) + b]du = \delta. \qquad (2)$$

Since the left-hand side is a continuously increasing function, there exists a time $t = t_1$, $t_0 < t_1$, such that the equation above holds. Similarly starting with $(y, z) = (\delta, b)$ at time t_1 the equation

$$\delta + \frac{1}{\kappa}\int_{t_1}^{t}[x(u) - b]du = -\delta \qquad (3)$$

is satisfied for some $t = t_2$, $t_1 < t_2$. Thus, the strictly increasing sequence $(t_k), k \in \mathbb{Z}$, defined by (1) uniquely describes the (output) function $z = z(t)$, for all $t,\ t \in \mathbb{R}$, and $|y| \le \delta$ by construction.

B. An Equivalent Circuit

By dividing with b on both sides of (1), we obtain

$$\int_{t_k}^{t_{k+1}} \frac{x(u)}{b}du = (-1)^k\left[-(t_{k+1} - t_k) + \frac{2\kappa\delta}{b}\right]$$

for all $k,\ k \in \mathbb{Z}$. Therefore, the increasing time sequence $(t_k), k \in \mathbb{Z}$, can be generated by an equivalent circuit with integration constant $\kappa = 1$ and a Schmitt trigger with parameters $\kappa\delta/b$ and 1 (see Fig. 3).

In what follows, without any loss of generality, a simple version of the TEM will be used. The input to the TEM is a bounded Lebesgues measurable function $x(t)$ with $|x(t)| \le c < 1$ for all $t, t \in \mathbb{R}$. The output of the TEM is a function z taking two
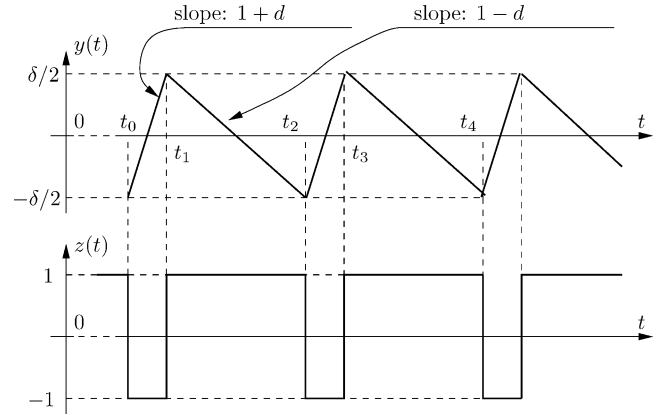

Fig. 4.   Time-domain illustration of the operation of the TEM with dc input.

values $z : \mathbb{R} \to \{-1, 1\}$ for all $t, t \in \mathbb{R}$, with transition times $(t_k), k \in \mathbb{Z}$, generated by the recursive equations

$$\int_{t_k}^{t_{k+1}} x(u)du = (-1)^k[\delta - (t_{k+1} - t_k)] \qquad (4)$$

for all $k,\ k \in \mathbb{Z}$, with δ measured in seconds. These equations map the amplitude information of the signal $x(t), t \in \mathbb{R}$, into the time sequence $(t_k), k \in \mathbb{Z}$. In what follows, the TEM consists of an integrator with integrator constant $\kappa = 1$ and Schmitt trigger with parameters $(\delta/2, 1)$.

Example: Assume that $x(t) = d$ (not necessarily positive), where d denotes a given DC level. For $d < -1$ or $d > 1$, the output of the integrator becomes unbounded, and thus, the overall TEM becomes unstable. This might lead to information loss because the output $z(t)$ can not track the input $x(t)$. If $|d| < 1$, the TEM is stable and (4) reduces to the simple recursion

$$t_{k+1} = t_k + \frac{\delta}{1 + (-1)^k d}$$

and, therefore, $t_{k+1} > t_k, k \in \mathbb{Z}$. Both $y(t)$ and $z(t)$ are periodic signals with period T and

$$T = t_{k+2} - t_k = \frac{2\delta}{1 - d^2} \qquad (5)$$

for all $k,\ k \in \mathbb{Z}$. The integrator output $y(t)$ and the overall output $z(t)$ are as shown in Fig. 4.

The mean value (the 0th-order Fourier-series coefficient) of $z(t)$ amounts to

$$\frac{(-1)^k[-(t_{k+1} - t_k) + (t_{k+2} - t_{k+1})]}{T} = d \qquad (6)$$

that is, the input and the output of the TEM have the same average value.

Note that the harmonics of $z(t)$ can be easily separated from the value corresponding to the dc input. Its fundamental frequency $1/T$ is inversely proportional to δ (the width of the hysteresis of the Schmitt trigger). Thus, if the maximum dc input signal is given, the minimum value for $1/T$ can be set by δ.

Corollary 1 (Upper and Lower Bounds for Trigger Times): For all input signals $x = x(t),\ t \in \mathbb{R}$, with

$|x(t)| \leq c < 1$, the distance between consecutive trigger times t_k and t_{k+1} is bounded by

$$\frac{\delta}{1+c} \leq t_{k+1} - t_k \leq \frac{\delta}{1-c} \tag{7}$$

for all k, $k \in \mathbb{Z}$.

Proof: Since $|x(t)| \leq c$, it is easy to see that

$$-c(t_{k+1} - t_k) \leq \int_{t_k}^{t_{k+1}} x(u)du \leq c(t_{k+1} - t_k). \tag{8}$$

By replacing the integral in the inequality above with its value given by (4) and solving for $t_{k+1} - t_k$ we obtain the desired result. The lower and upperbounds are achieved for a constant input $x(t) = c$, for all t, $t \in \mathbb{R}$, for k even and odd, respectively. A similar relation applies when $x(t) = -c$, for all t, $t \in \mathbb{R}$.

Remark 2: If $x(t)$ is a continuous function, by the mean value theorem there exists a $\xi_k \in [t_k, t_{k+1}], k \in \mathbb{Z}$, such that

$$x(\xi_k)(t_{k+1} - t_k) = (-1)^k[\delta - (t_{k+1} - t_k)] \tag{9}$$

i.e., the sample $x(\xi_k)$ can be explicitly recovered from information contained in the process $z(t)$, $t_k \leq t \leq t_{k+1}, k \in \mathbb{Z}$. Intuitively, therefore, any class of input signals that can be recovered from its samples can also be recovered from $z(t)$.

III. PERFECT RECOVERY

A TDM has the task of recovering the signal $x = x(t), t \in \mathbb{R}$, from $z = z(t), t \in \mathbb{R}$, or a noisy version of the same. Here, we will focus on the recovery of the original signal x based on z only. We shall show that a perfect recovery is possible, that is, the input signal x can be recovered from z without any loss of information.

A. Recovery Algorithms

Informally, a function of the length of the interval between two consecutive trigger times of $z(t)$ provides an estimate of the integral of $x(t)$ on the same interval. This estimate used in conjunction with the bandlimited assumption on x enables a perfect reconstruction of the signal even though the trigger times are irregular. In order to achieve perfect reconstruction, the distance between two consecutive trigger times has to be, in average [7] smaller than the distance between the uniformly spaced samples in the classical sampling theorem [9], [18].

The mathematical methodology used here for deriving recovery algorithms is based on the theory of frames [4]. We shall construct an operator on $L^2(\mathbb{R})$, the space of square integrable functions defined on $\mathbb{R}$, and by starting from a good initial guess followed by successive interations, obtain sucessive approximations that converge in the appropriate norm to the original signal x.

Let us assume that $x = x(t), t \in \mathbb{R}$, with $|x(t)| \leq c < 1$, is a finite energy signal on $\mathbb{R}$ bandlimited to $[-\Omega, \Omega]$ and let the operator $\mathcal{A}$ be given by

$$\mathcal{A}x = \sum_{k \in \mathbb{Z}} \int_{t_k}^{t_{k+1}} x(u)du \, g(t - s_k)$$

$$= \sum_{k \in \mathbb{Z}} (-1)^k[\delta - (t_{k+1} - t_k)] \, g(t - s_k)$$

where $g(t) = \sin(\Omega t)/\pi t$ and $s_k = (t_{k+1} + t_k)/2$. The values of $(\int_{t_k}^{t_{k+1}} x(u)du), k \in \mathbb{Z}$, are obtained from the sequence $(t_k), t \in \mathbb{Z}$, available at the TDM, through (4).

The realization of the operator $\mathcal{A}$ above is highly intuitive. Dirac-delta pulses generated at times s_k with weight $\int_{t_k}^{t_{k+1}} x(u)du = (-1)^k[\delta - (t_{k+1} - t_k)]$ are passed through an ideal low-pass filter with unity gain for $\omega \in [-\Omega, \Omega]$ and zero otherwise.

Let $x_l = x_l(t), t \in \mathbb{R}$, be a sequence of bandlimited functions defined by the recursion

$$x_{l+1} = x_l + \mathcal{A}(x - x_l) \tag{10}$$

for all l, $l \in \mathbb{N}$, with the initial condition $x_0 = \mathcal{A}x$.

The operator $\mathcal{A}^*$ defined by

$$\mathcal{A}^*x = \sum_{k \in \mathbb{Z}} x(s_k)f_k(t) \tag{11}$$

where $f_k(t) = (g * 1_{[t_k, t_{k+1}]})(t)$ represents the output of a low-pass filter with impulse response g (that is, the $*$ denotes the convolution operation) whose input is the pulse of finite width $1_{[t_k, t_{k+1}]}(t)$. We note the following [5].

Lemma 2: $\mathcal{A}$ and $\mathcal{A}^*$ are adjoint operators.

Proof: See Appendix, Section B.

Note that since the distance between two consecutive trigger times is bounded from above by $\delta/(1-c)$ [see (7)].

Lemma 3:

$$\|I - \mathcal{A}\| \leq r$$

where I is the identity operator and $r = (\delta/(1-c))(\Omega/\pi)$.

Proof: See Appendix B. The original proof appeared in [5].

Theorem 1 (Operator Formulation): Let $x = x(t), t \in \mathbb{R}$ be a bounded signal $|x(t)| \leq c < 1$ bandlimited to $[-\Omega, \Omega]$. Let $z = z(t), t \in \mathbb{R}$, be the ouput of a TEM with integrator constant $\kappa = 1$ and Schmitt trigger parameters $(\delta/2, 1)$. If $\delta < (1 - c)\pi/\Omega$, the signal x can be perfectly recovered from its associated trigger times $(t_k), k \in \mathbb{Z}$, as

$$\lim_{l \to \infty} x_l(t) = x(t)$$

and

$$\|x - x_l\| \leq r^{l+1}\|x\|.$$

Proof: By induction, we can show that

$$x_l = \sum_{k=0}^{l} (I - \mathcal{A})^k \mathcal{A}x.$$

Since $\|I - \mathcal{A}\| \leq r < 1$

$$\lim_{l \to \infty} x_l = \sum_{k \in \mathbb{N}} (I - \mathcal{A})^k \mathcal{A}x = \mathcal{A}^{-1}\mathcal{A}x = x$$

where $\mathbb{N}$ denotes the set of nonnegative integers. Also

$$x - x_l = \sum_{k \geq l+1} (I - \mathcal{A})^k \mathcal{A}x = (I - \mathcal{A})^{l+1} \sum_{k \in \mathbb{N}} (I - \mathcal{A})^k \mathcal{A}x$$

$$= (I - \mathcal{A})^{l+1} \mathcal{A}^{-1}\mathcal{A}x = (I - \mathcal{A})^{l+1}x$$

and, therefore, $\|x - x_l\| \leq r^{l+1}\|x\|$.

Remark 3: The most general recovery result only requires that the average number of trigger times is bounded by the inverse of the Nyquist rate [7]. However, this result lacks operational significance in our setting.

Let us define the vectors $\mathbf{g} = [g(t - s_k)]$, $\mathbf{q} = [(-1)^k[\delta - (t_{k+1} - t_k)]]$ and the matrix $\mathbf{G} = [G_{lk}] = [\int_{t_l}^{t_{l+1}} g(u - s_k)\, du]$; $\mathbf{I}$ denotes the identity matrix and T the (matrix) transpose. We have the following.

Corollary 2 (Matrix Formulation): Under the assumptions of Theorem 1, the bandlimited signal x can be perfectly recovered from its associated trigger times $(t_k), k \in \mathbb{Z}$, as

$$x(t) = \lim_{l \to \infty} x_l(t) = \mathbf{g}^T \mathbf{G}^+ \mathbf{q} \qquad (12)$$

where $\mathbf{G}^+$ denotes the pseudoinverse of $\mathbf{G}$. Furthermore

$$x_l(t) = \mathbf{g}^T \mathbf{P}_l \mathbf{q} \qquad (13)$$

where $\mathbf{P}_l$ is given by

$$\mathbf{P}_l = \sum_{k=0}^{l} (\mathbf{I} - \mathbf{G})^k. \qquad (14)$$

Proof: By induction

$$x_0(t) = \mathcal{A}x = \sum_{k \in \mathbb{Z}} \int_{t_k}^{t_{k+1}} x(u)du\, g(t - s_k) = \mathbf{g}^T \mathbf{q}. \quad (15)$$

Assume that $x_l(t) = \mathbf{g}^T \mathbf{P}_l \mathbf{q}$ with $\mathbf{P}_l = \sum_{k=0}^{l} (\mathbf{I} - \mathbf{G})^k$. We have

$$\begin{aligned}
x_{l+1}(t) &= x_l + \mathcal{A}(x - x_l) \\
&= \mathbf{g}^T (\mathbf{P}_l + \mathbf{I} - \mathbf{G}\mathbf{P}_l)\mathbf{q} = \mathbf{g}^T \mathbf{P}_{l+1} \mathbf{q}.
\end{aligned}$$

Finally, the equality

$$x(t) = \lim_{l \to \infty} x_l(t) = \lim_{l \to \infty} \mathbf{g}^T \mathbf{P}_l \mathbf{q} = \mathbf{g}^T \mathbf{G}^+ \mathbf{q}$$

is guaranteed by Theorem 1 where $\mathbf{G}^+$ is the pseudoinverse of $\mathbf{G}$ (see [19] for more details).

Remark 4: If $\mathbf{c} = [c_k]$ is the vector defined by $\mathbf{c} = \mathbf{G}^+ \mathbf{q}$ then the recovery formula (12) becomes

$$x(t) = \sum_{k \in \mathbb{Z}} c_k g(t - s_k).$$

Therefore, the recovery algorithm given by (12) has a very simple interpretation. Dirac-delta pulses generated at times s_k with weight c_k are passed through a low-pass filter with unity gain on $[-\Omega, \Omega]$ and zero otherwise. For a precise definition and motivation of the pseudoinverse the reader is referred to [19].

Remark 5: While deceptively simple, the signal recovery formula exposed in (12) hides the nonlinear relationship between the bandlimited signal $x = x(t), t \in \mathbb{R}$, and the trigger times $(t_k), k \in \mathbb{Z}$. Note however, that the signal $x = x(t), t \in \mathbb{R}$, is a function of the time sequence $(t_k), k \in \mathbb{Z}$, through the pseudoinverse of $\mathbf{G}$. Clearly, linear operations on the TEM input signal do not translate, in general, into linear operations on the (output) trigger times.
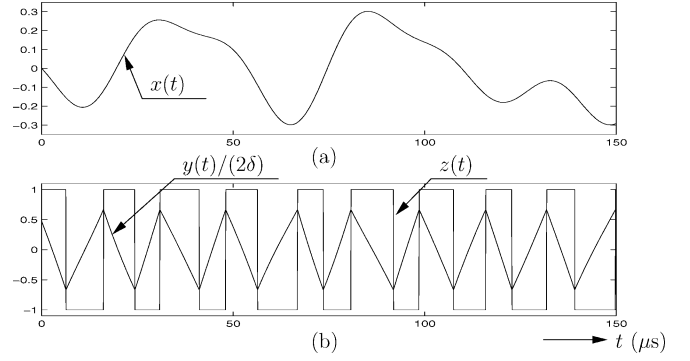

Fig. 5. Input signal $x(t)$ (a), integrator and TEM output $y(t)$ and $z(t)$ (b).
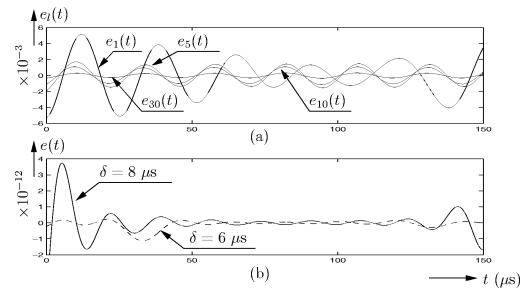

Fig. 6. Approximating signals using iteration (a), overall error signals using closed formulas (b).

B. Example

The mathematical formulation of the previous section assumes that the dimensionality of the matrices and vectors used is infinite. In simulations, however, only a finite time window can be used. We briefly investigate two different implementations of the TDM in the finite dimensional case that are, respectively, based on the recursive (13) and the closed form formula (12).

In all our simulations, the input signal is given by $x(t) = \sum_{k \in \mathbb{Z}} x(kT)g(t - kT)$ where the samples $x(T)$ through $x(12T)$, are respectively, -0.1961, $0.186\,965$, $0.207\,271$, $0.098\,773\,6$, $-0.275\,572$, $0.020\,166\,5$, $0.290\,247$, $0.138\,374$, $-0.067\,588$, $-0.145\,661$, $-0.111\,33$, $-0.291\,498$, $x(kT) = 0$, for $k \leq 0$ and $k > 12$; $c = .3$, $\Omega = 2\pi \cdot 40$ kHz and $T = \pi/\Omega = 12.5$ μs. The evaluation of the trigger times was carried out in the interval $-2T \leq t \leq 15T$. Fig. 5(a) shows $x(t)$ together with the time window used for simulations. Fig. 5(b) shows the simulation results for $y(t)$ and $z(t)$ with $\delta = 8$ μs. The 26 trigger times of $z(t)$ (only 18 are shown) were determined with high accuracy using (4).

1) The error signals shown by Fig. 6(a) are defined as $e_l = e_l(t) = x_l(t) - x(t)$, where $x_l(t)$ was calculated based on (13). Instead of applying (14) directly we used the recursion $\mathbf{P}_{l+1} = \mathbf{I} + \mathbf{P}_l(\mathbf{I} - \mathbf{G})$ and calculated $x_l(t)$ iteratively. As shown, $e_l(t)$ decreases in agreement with Theorem 1, since with the parameters introduced $r = 0.914 < 1$.

2) Although the matrix $\mathbf{G}$ in (12) is ill-conditioned, perfect recovery can be achieved using $\mathbf{G}^+$, the pseudoinverse of

G (if **G** is nonsingular then $\mathbf{G}^+ = \mathbf{G}^{-1}$). The corresponding error signal defined as $e(t) = \mathbf{g}^T \mathbf{G}^+ \mathbf{q} - x(t)$ is shown Fig. 6(b) for $\delta = 8 \ \mu s$ ($r = 0.914$ for the solid line) and $\delta = 6 \ \mu s$ ($r = 0.616$ for the dashed line). The improvement of the RMS is about 10 dB. The remaining small error is due to i) the finite precision used, and 2) the finite time window employed.

IV. RELATIONSHIP TO IRREGULAR SAMPLING AND OTHER MODULATION SCHEMES

A. Relationship to Irregular Sampling

In this section, we highlight the relationship between time encoding and irregular sampling, i.e., between two information representations of a bandlimited signal as a discrete time and a discrete amplitude sequence. As in the previous sections $x = x(t), t \in \mathbb{R}$, shall denote a bounded signal $|x(t)| \le c < 1$ bandlimited to $[-\Omega, \Omega]$. The time sequence will be denoted by $(t_k), k \in \mathbb{Z}$, and the irregular samples $(x(s_k)), k \in \mathbb{Z}$, are available at times $(s_k), \ k \in \mathbb{Z}$.

In Theorem 2 below, $x_l = x_l(t), t \in \mathbb{R}$, will denote a sequence of bandlimited functions defined by the recursion

$$x_{l+1} = x_l + \mathcal{A}^*(x - x_l) \tag{16}$$

for all l, $l \in \mathbb{N}$, with the initial condition $x_0 = \mathcal{A}^* x$. The relevance of $\mathcal{A}^*$ in our context is provided by the following theorem [5].

Theorem 2 (Reconstruction From Irregular Samples): If $r = \delta/(1 - c) \cdot \Omega/\pi < 1$ the bandlimited signal x can be perfectly recovered from its samples $(x(s_k)), k \in \mathbb{Z}$, as

$$\lim_{l \to \infty} x_l(t) = x(t)$$

and

$$\|x - x_l\| \le r^{l+1} \|x\|.$$

Proof: The proof is based on the proof of Lemma 3 in the Appendix . The original proof appeared in [5], Theorem 5.

Let us define $\mathbf{f} = [f_k(t)]$, $\mathbf{x} = [x(s_k)]$ and $\mathbf{F} = [F_{lk}] = [f_k(s_l)]$ (see also (14)). We have the following.

Corollary 3 (Matrix Recovery From Irregular Samples): Under the assumptions of Theorem 2 the bandlimited signal x can be perfectly recovered from its samples $(x(s_k)), k \in \mathbb{Z}$, as

$$x(t) = \lim_{l \to \infty} x_l(t) = \mathbf{f}^T \mathbf{F}^+ \mathbf{x} \tag{17}$$

where $\mathbf{F}^+$ denotes the pseudoinverse of $\mathbf{F}$. Furthermore

$$x_l(t) = \mathbf{f}^T \mathbf{P}_l \mathbf{x} \tag{18}$$

where $\mathbf{P}_l$ is given by

$$\mathbf{P}_l = \sum_{k=0}^{l} (\mathbf{I} - \mathbf{F})^k. \tag{19}$$

Proof: The proof closely follows Corollary 2.

Remark 6: While we have highlighted the similarities between time encoding and irregular sampling from the algorithmic recovery point of view, there are also substantial differences between the two. One key difference mentioned here derives from the functional relationship between the trigger times $(t_k), k \in \mathbb{Z}$, and the associated time sequence $(s_k), k \in \mathbb{Z}$ on the one hand and the bandlimited signal on the other. In the case of time encoding, the t_k's are signal dependent. This is clearly underscored by (4). For irregular sampling, however, the s_k's are signal independent.

B. Relationship to Other Modulation Schemes

The TDM and the demodulator for frequency modulation (FM) [2] operate on a signal that has the same information structure. Recall that FM demodulation is achieved by finding the times t such that

$$\sin\left(\omega t + \eta \int_{t_0}^{t} x(u) du + \phi\right) = 0$$

where ω is the modulation frequency and η is the modulation index. Therefore,

$$\int_{t_k}^{t_{k+1}} x(u) du = -\frac{\omega}{\eta}(t_{k+1} - t_k) + \frac{\pi}{\eta}.$$

We call the mapping of amplitude information into timing information as exemplified by the (1), (4) and (34) the transylvania transform or t-transform for short. Note that the (1), (4) and (35) have the same basic structure. Hence, an FM modulated signal x can be perfectly recovered from the sequence of times $(t_k), k \in \mathbb{Z}$ using the TDM. These observations establish a bridge to nonuniform sampling methods previously applied to improve the performance of FM and other nonlinear modulators[14].

The TEM also models an asynchronous sigma–delta modulator [8] and, therefore, the latter is invertible. Past attempts at building sigma–delta demodulators have led to low accuracy in signal recovery [16]. This is because of the linear structure of these demodulators.

Finally, we note that bandlimited stimuli (signals) encoded with an integrate-and-fire neuron with an absolute refractory period can be recovered loss-free from its neural spike train at its output. The algorithm for perfect recovery and conditions for its convergence are given in [12].

V. RECOVERY SENSITIVITY WITH RESPECT TO δ

In this section, we will first demonstrate the high sensitivity of the perfect recovery algorithm with respect to implementation errors of the parameter δ in the TDM. We will then demonstrate how this can be overcome and advance an δ-insensitive recovery algorithm.

We would like to note here that sensitivity issues also arise in the TEM. For example, the Schmitt trigger's implementation might assign the value $1 + \varepsilon$ to the upper threshold and
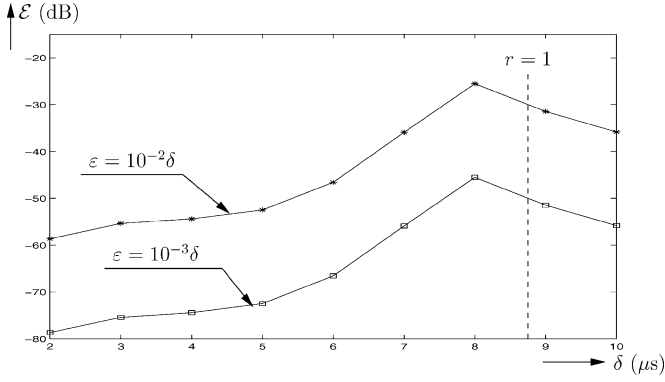
Fig. 7. Dependence of $\mathcal{E}$ in decibels on δ parameterized by $\varepsilon = 10^{-2}\delta$ (stars) and $\varepsilon = 10^{-3}\delta$ (squares).

$-1 + \varepsilon$ to the lower threshold. Therefore, the recursive equation describing the TEM becomes

$$\int_{t_k}^{t_{k+1}} [x(u) - \varepsilon]du = (-1)^k[\delta - (t_{k+1} - t_k)]$$

for all k, $k \in \mathbb{Z}$. As a result, $x(t) - \varepsilon$ is recovered instead of $x(t)$. A small dc bias ε is often times acceptable in practice.

A. δ With a Fixed Error ε at the TDM

The model considered in this section is based on the premise that the TEM is employing δ and the TDM implements $\delta + \varepsilon$ and has exact knowledge of the trigger times. The reconstruction algorithm consistently generates an error signal e given by

$$e(t) = x(t) - \hat{x}(t) = \sum_{k \in \mathbb{N}} (I - \mathcal{A})^k \varepsilon \sum_{l \in \mathbb{Z}} g(t - s_l)$$

where $\hat{x}$ is the output of a TDM that uses $\delta + \epsilon$ for recovery.

In what follows, we define an MSE measure $\mathcal{E}^2$ as

$$\mathcal{E}^2 = \lim_{n \to \infty} \frac{1}{2nT_{\min}} \|e1_{[-nT_{\min}, nT_{\min}]}\|^2$$

where $1_{[-nT_{\min}, nT_{\min}]}$ denotes a pulse of finite width and magnitude one (i.e., an indicator function)

$$\|e1_{[-nT_{\min}, nT_{\min}]}\|^2 = \int_{\mathbb{R}} e^2(u)1_{[-nT_{\min}, nT_{\min}]}(u)du$$

and $T_{\min} = \min_{k \in \mathbb{Z}} T_k$ with $T_k = t_{k+1} - t_k$.

Example: A sample of the dependance of the mean-square recovery error on δ parameterized by ε is shown in Fig. 7. In all figures, the notation $\mathcal{E}$[dB] stands for $10 \times \lg(\mathbb{E}[\mathcal{E}^2])$. Note also that in all our simulations, the input signal was identical to the one described in Section III.B.

B. δ-Insensitive Recovery Algorithm

As shown in Fig. 7, the implementation of the TDM recovery algorithm given in Theorem 1, is highly sensitive to the exact knowledge of the parameter δ. The remedy is provided by the following

Lemma 4 (The Compensation Principle):

$$\int_{t_l}^{t_{l+2}} x(u)du = (-1)^l[(t_{l+2} - t_{l+1}) - (t_{l+1} - t_l)]$$

for all $l \in \mathbb{Z}$.

Proof: The desired result is obtained by adding (4) for $k = l$ and $k = l + 1$.

Remark 7: Note that the compensation principle provides for an estimate of the amplitude of the input signal $x(t)$ that does not explicitly depend on δ. Note also that the compensation principle can be easily extended to subsets of the real line or to the entire real line. Thus, the dc component of the input can be recovered from $z(t)$ even for nonbandlimited input signals $x(t), t \in \mathbb{R}$.

The compensation principle suggests the construction of an operator of the form

$$\mathcal{B}x = \sum_{k \in \mathbb{Z}} \int_{t_k}^{t_{k+2}} x(u)du \, f_{k+1}(t)$$
$$= \sum_{k \in \mathbb{Z}} \int_{t_k}^{t_{k+1}} x(u)du \, [f_k(t) + f_{k+1}(t)].$$

The exact form of the functions f_k will be described below. The operators $\mathcal{A}$ and $\mathcal{B}$ are identical provided that $f_k(t) + f_{k+1}(t) = g(t - s_k)$, for all $t \in \mathbb{R}$ and $k \in \mathbb{Z}$, or in matrix form

$$\mathbf{g} = \mathbf{B}^T \mathbf{f}$$

where $\mathbf{f} = [f_k]$ and the elements of the matrix $\mathbf{B} = [B_{kl}]$ are given by $B_{kl} = 1$ for $k = l$ or $k = l + 1$ and zero otherwise. Note that, the inverse of $\mathbf{B}$ is given by $B_{kl}^{-1} = (-1)^{k-l}$ for $k \geq l$ and zero otherwise. Note also that

$$\mathbf{Bq} = [(-1)^k(t_{k+2} - 2t_{k+1} + t_k)]$$

does not explicitly depend on δ.

Let $x_l = x_l(t), t \in \mathbb{R}$, be a sequence of bandlimited functions defined by the recursion

$$x_{l+1} = x_l + \mathcal{B}(x - x_l) \qquad (20)$$

for all l, $l \in \mathbb{N}$, with the initial condition $x_0 = \mathcal{B}x$.

Theorem 3 (δ-Insensitive Recovery Algorithm–Operator Form): If $r = \delta/(1 - c) \cdot \Omega/\pi < 1$, the bandlimited signal x can be perfectly recovered from its associated trigger times $(t_k), k \in \mathbb{Z}$, without explicit knowledge of the parameter δ as

$$x(t) = \lim_{l \to \infty} x_l(t). \qquad (21)$$

Furthermore

$$\|x - x_l\| \leq r^{l+1}\|x\|.$$

Proof: Since $\mathcal{A} = \mathcal{B}$ this above result is the same as the one of Theorem 1.

Corollary 4 (δ-Insensitive Recovery Algorithm—Matrix Form): If $r = \delta/(1-c) \cdot \Omega/\pi < 1$, the bandlimited signal x can be perfectly recovered from its associated trigger times $(t_k), k \in \mathbb{Z}$, without explicit knowledge of the parameter δ as

$$x(t) = \lim_{l \to \infty} x_l(t) = \mathbf{g}^T \cdot \mathbf{B}^{-1}(\mathbf{BGB}^{-1})^+ \cdot \mathbf{Bq}. \qquad (22)$$

Furthermore,

$$x_l(t) = \mathbf{g}^T \cdot \mathbf{B}^{-1}\mathbf{Q}_l \cdot \mathbf{Bq},$$

where $\mathbf{Q}_l$ is given by

$$\mathbf{Q}_l = \sum_{k=0}^{l} [\mathbf{I} - \mathbf{BGB}^{-1}]^k.$$

Proof: Using the notation of Theorem 2, x_l can be rewritten as

$$x_l(t) = \mathbf{g}^T \mathbf{P_l q} = \mathbf{g}^T \cdot \mathbf{B}^{-1}(\mathbf{BP_l B}^{-1}) \cdot \mathbf{Bq}.$$

Since

$$\mathbf{BP_l B^{-1}} = \mathbf{B} \sum_{k=0}^{l} (\mathbf{I} - \mathbf{G})^k \mathbf{B^{-1}} = \sum_{k=0}^{l} (\mathbf{I} - \mathbf{BGB^{-1}})^k$$

we have

$$x(t) = \lim_{l \to \infty} \mathbf{g}^T \cdot \mathbf{B}^{-1} \sum_{k=0}^{l} (\mathbf{I} - \mathbf{BGB^{-1}})^k \cdot \mathbf{Bq}$$
$$= \mathbf{g}^T \cdot \mathbf{B}^{-1}(\mathbf{BGB^{-1}})^+ \cdot \mathbf{Bq}.$$

Remark 8: Note that (22) can be rewritten as

$$x(t) = \mathbf{f}^T \mathbf{F}^+ \cdot \mathbf{Bq}$$

where $\mathbf{F} = [F_{lk}] = [\int_{t_l}^{t_{l+2}} f_k(u)du]$. Therefore, the representation of x in (22) lends itself to a simple interpretation akin the one in Remark 3. Alternatively, a representation of the form $x(t) = \mathbf{g}^T (\mathbf{BG})^+ \cdot \mathbf{Bq}$ can be employed that is directly based on the basis functions $\mathbf{g}$.

Example: The δ-insensitive recovery algorithm achieves perfect recovery provided that $r < 1$. Simulation results for the δ-sensitive and δ-insensitive recovery algorithms are shown in Fig. 8 and are denoted by stars and squares, respectively. The dotted vertical line corresponds to the value of δ for which $r = 1$. The difference between the MSEs plotted in Fig. 8 is due to the removal of the first row of the matrix $\mathbf{B}$ and the last column of its inverse. Through this simple truncation procedure the compensation priniciple remains valid.

VI. RECOVERY SENSITIVITY WITH RESPECT TO TIME QUANTIZATION

Here, we shall assume that the sequence of trigger times $(t_k), k \in \mathbb{Z}$, is measured with finite precision and the actual values available for recovery are $\hat{t}_k, k \in \mathbb{Z}$. We shall denote by $T_k = t_{k+1} - t_k$ and $\hat{T}_k = \hat{t}_{k+1} - \hat{t}_k$ for all $k \in \mathbb{Z}$.
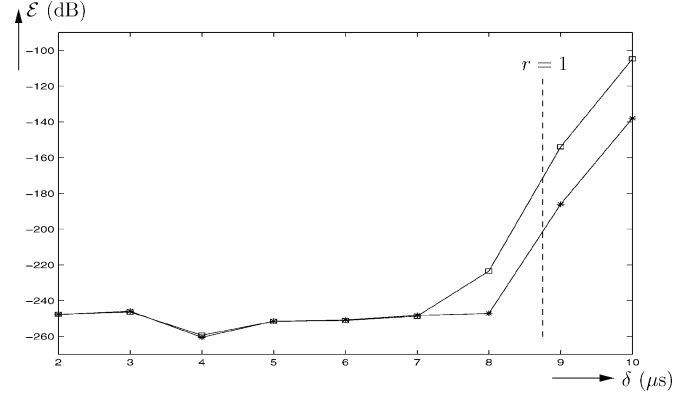

Fig. 8. MSE in decibels for the δ-sensitive (stars) and δ-insensitive algorithms (squares).

A. Upper Bound on a Measure of Error Recovery

The key point of our analysis is the observation that, if the condition $\max_k \hat{T}_k < T$ is satisfied, then

$$x = \sum_{k \in \mathbb{N}} (I - \hat{\mathcal{A}})^k \hat{\mathcal{A}} x$$

where $\hat{\mathcal{A}}$ is defined by

$$\hat{\mathcal{A}} x = \sum_{k \in \mathbb{Z}} \int_{\hat{t}_k}^{\hat{t}_{k+1}} x(u) du \, g(t - \hat{s}_k) \qquad (23)$$

and $\hat{s}_k = (\hat{t}_k + \hat{t}_{k+1})/2$. Note that this results holds for any time sequence whose consecutive intervals are lower bounded and whose average is upperbounded by the Nyquist rate [7]. Since the reconstructed signal is given by

$$\hat{x} = \sum_{k \in \mathbb{N}} (I - \hat{\mathcal{A}})^k \sum_{l \in \mathbb{Z}} [(-1)^l (\delta - \hat{T}_l)] g(t - \hat{s}_l)$$

the error signal amounts to

$$e(t) = \sum_{k \in \mathbb{N}} (I - \hat{\mathcal{A}})^k \sum_{l \in \mathbb{Z}} \epsilon_l g(t - \hat{s}_l) \qquad (24)$$

where [see also, (4)]

$$\epsilon_k = (-1)^k (\delta - \hat{T}_k) - \int_{\hat{t}_k}^{\hat{t}_{k+1}} x(u) du. \qquad (25)$$

Proposition 1: Assuming that the quantization error $d_k = \hat{T}_k - T_k, k \in \mathbb{Z}$, is a sequence of i.i.d. random variables on $[-\Delta/2, \Delta/2]$, the expected MSE is bounded by

$$\mathbb{E}[\mathcal{E}^2] \leq \frac{1+c}{T\delta} \cdot \left(\frac{1+c}{1-r}\right)^2 \cdot \frac{\Delta^2}{12} \qquad (26)$$

where $\mathbb{E}$ denotes the expectation (mean value).

Remark 9: Conditions for modeling the quantization error as an independent identically distributed (i.i.d.) sequence appear in the classic papers [3] and [17]. For an alternative analysis to the one presented here, see [16].

Proof: We note that with $w_n(t) = 1_{[-nT_{\min}, nT_{\min}]}(t)$

$$
\mathcal{E}^2 = \lim_{n \to \infty} \frac{1}{2nT_{\min}} \left\| \sum_{k \in \mathbb{N}} (I - \mathcal{A})^k \sum_{l \in \mathbb{Z}} \epsilon_l g(t - s_l) \cdot w_n(t) \right\|^2
$$

$$
\leq \left\| \sum_{k \in \mathbb{N}} (I - \mathcal{A})^k \right\|^2 \lim_{n \to \infty} \frac{\left\| \sum_{l \in \mathbb{Z}} \epsilon_l g(t - s_l) \cdot w_n(t) \right\|^2}{2nT_{\min}}
$$

$$
\leq \frac{1}{(1-r)^2} \lim_{n \to \infty} \frac{1}{2nT_{\min}} \left\| \sum_{l \in \mathbb{N}} \epsilon_l g(t - \hat{s}_l) \cdot w_n(t) \right\|^2. \quad (27)
$$

Since the norm above is increasing in n

$$
\mathbb{E}[\mathcal{E}^2] \leq \frac{1}{(1-r)^2} \lim_{n \to \infty} \frac{1}{2nT_{\min}} \mathbb{E} \left\| \sum_{l \in \mathbb{N}} \epsilon_l g(t - \hat{s}_l) \cdot w_n(t) \right\|^2. \tag{28}
$$

The expectation on the right-hand side can be bounded as follows:

$$
\mathbb{E} \left\| \sum_{l \in \mathbb{N}} \epsilon_l g(t - \hat{s}_l) \cdot 1_{[-nT_{\min}, nT_{\min}]}(t) \right\|^2
$$

$$
= \int_{-nT_{\min}}^{nT_{\min}} \sum_{k \in \mathbb{Z}} \sum_{m \in \mathbb{Z}} g(t - \hat{s}_k) g(t - \hat{s}_m) dt \cdot \mathbb{E}[\epsilon_k \epsilon_m]
$$

$$
= \int_{-nT_{\min}}^{nT_{\min}} \sum_{k \in \mathbb{Z}} g^2(t - \hat{s}_k) dt \cdot \left(\frac{\delta}{T_k} \right)^2 \frac{\Delta^2}{12} \leq \frac{2n}{T} \cdot (1 + c)^2 \cdot \frac{\Delta^2}{12} \tag{29}
$$

since

$$
\mathbb{E}[\epsilon_k \epsilon_m] = \left(\frac{\delta}{T_k} \right)^2 \frac{\Delta^2}{12} \delta_{k,m} \tag{30}
$$

and

$$
\frac{1}{2n} \int_{-nT_{\min}}^{nT_{\min}} \sum_{k \in \mathbb{Z}} g^2(t - \hat{s}_k) dt \leq \frac{1}{T}
$$

as shown in the Result 4 and 3, respectively, in the Appendix . Finally, substituting the upperbound derived in (29) into (28) gives the desired result.

B. Uniform Sampling Approximation

The expected MSE can be explicilty evaluated when the quantized trigger times are uniformly spaced. The result below is a gauge for evaluating the recovery error of time encoded bandlimited signals.

Proposition 2: Assuming that the quantization error $d_k = \hat{T}_k - T_k, k \in \mathbb{Z}$, is a sequence of i.i.d. random variables on $[-\Delta/2, \Delta/2]$, and the t_k's are uniformly spaced, the expected MSE is given by

$$
\mathbb{E}[\mathcal{E}^2] = \frac{1}{2\pi} \frac{\Delta^2}{12} \frac{\delta^2}{S^3} \int_{-\Omega}^{\Omega} \left| \frac{\frac{\omega S}{2}}{\sin\left(\frac{\omega S}{2} \right)} \right|^2 d\omega \tag{31}
$$

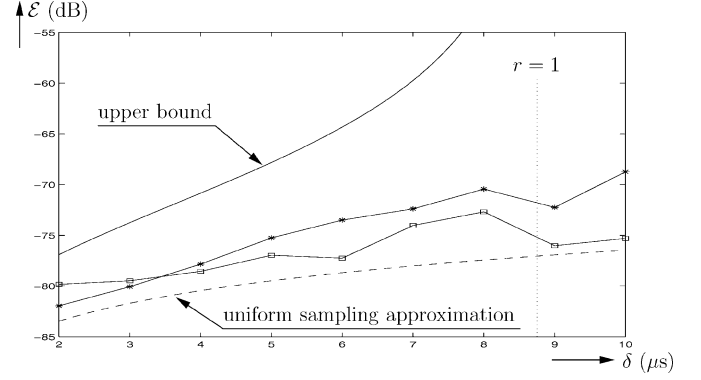where $S = \hat{t}_{k+1} - \hat{t}_k$ for all k, $k \in \mathbb{Z}$.

Fig. 9. Dependence of $\mathcal{E}$ in decibels on δ for time encoding (stars) and irregular sampling (squares) for $N = 10$.
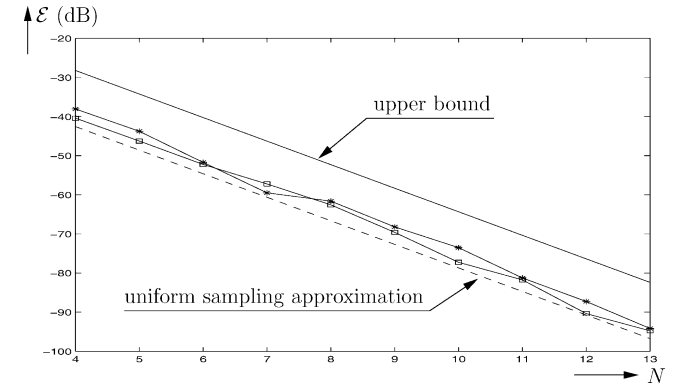

Fig. 10. Dependence of $\mathcal{E}$ in decibels on the number of quantization bits N for time encoding (stars) and irregular sampling (squares) for $\delta = 6\,\mu$s.

Proof: The expression above can be obtained from Result 5 in the Appendix by taking the inverse Fourier transform on both sides of equality (46) and setting $\tau = 0$.

C. Example

Figs. 9 and 10 show the mean-square recovery error $\mathcal{E}$ in decibels as a function of δ and the number of quantization bits, N, respectively. The same figures also depict the upperbound arising in inequality (26) as well the uniform sampling approximation (31). All other parameters in the simulation are as described in the Example of Section III-B. More details about these figures are given in Section VII.

VII. COMPARISON OF TIME AND AMPLITUDE QUANTIZATION

Here, we shall compare the effects of quantization in the time and amplitude domains. Since time encoding and irregular sampling are different discrete representations of information contained in a bandlimited function, signal recovery from a quantized version of the trigger times and irregular samples, respectively, is of great interest in practice.

A. Signal Recovery From Irregular Samples

In [11], we have established the relationship between time encoding and irregular sampling. Here, we shall employ an alternative signal recovery method from its irregular samples originally developed in [5].

In what follows we shall use the operator $\mathcal{S}$ defined by

$$\mathcal{S}x = \frac{1}{1+r^2} \cdot \frac{\Omega}{\pi} \sum_{k \in \mathbb{Z}} T_k x(s_k) g(t - s_k)$$

where $T_k = t_{k+1} - t_k$, for all $k, k \in \mathbb{Z}$. Also, $x_l = x_l(t), t \in \mathbb{R}$, will denote a sequence of bandlimited functions defined by the recursion

$$x_{l+1} = x_l + \mathcal{S}(x - x_l) \qquad (32)$$

for all l, $l \in \mathbb{N}$, with the initial condition $x_0 = \mathcal{S}x$. The relevance of $\mathcal{S}$ in our context is provided by the following theorem [5].

Theorem 4 (Reconstruction From Irregular Samples): If $r = \delta/(1-c) \cdot \Omega/\pi < 1$, the bandlimited signal x can be perfectly recovered from its samples $(x(s_k)), k \in \mathbb{Z}$, as

$$\lim_{l \to \infty} x_l(t) = x(t)$$

and

$$\|x - x_l\| \le \left(\frac{2r}{1+r^2} \right)^{l+1} \|x\|.$$

Proof: See [5, , Th. 6].

Let us define $\mathbf{g} = [g(t - s_k)]$, $\mathbf{p} = [T_k x(s_k)]$ and $\mathbf{H} = [H_{lk}] = [T_l g(s_l - s_k)]$. We have the following.

Corollary 5 (Matrix Recovery From Irregular Samples): Under the assumptions of Theorem 3 the bandlimited signal x can be perfectly recovered from its samples $(x(s_k)), k \in \mathbb{Z}$, as

$$x(t) = \lim_{l \to \infty} x_l(t) = \mathbf{g}^T \mathbf{H}^+ \mathbf{p} \qquad (33)$$

where $\mathbf{H}^+$ denotes the pseudoinverse of $\mathbf{H}$. Furthermore

$$x_l(t) = \mathbf{g}^T \mathbf{P}_l \mathbf{p} \qquad (34)$$

where $\mathbf{P}_l$ is given by

$$\mathbf{P}_l = \sum_{k=0}^{l} (\mathbf{I} - \mathbf{H})^k. \qquad (35)$$

Proof: The proof closely follows Corollary 2.

B. Upperbound for the Amplitude Quantization Error

Assume that the instances s_k are exactly known and the amplitudes $x(s_k)$ are corrupted to $x(s_k) + \epsilon_k$.

Proposition 3: If the random variables $(\epsilon_k), k \in \mathbb{Z}$, are independent uniformly distributed within $[-\varepsilon/2, \varepsilon/2]$ then

$$\mathbb{E}[\mathcal{E}^2] \le \frac{r}{(1-r)^2} \frac{1+c}{1-c} \frac{\varepsilon^2}{12}. \qquad (36)$$

Proof: The error signal due to amplitude quantization is

$$e(t) = \hat{x}(t) - x(t) = \sum_{k=0}^{\infty} (I - \mathcal{S})^k \sum_{l \in \mathbb{Z}} T_l \epsilon_l g(t - s_l).$$

Following the same derivation as in Proposition 2, we obtain

$$\mathbb{E}[\mathcal{E}^2] \le \frac{1}{(1-r)^2} \frac{T_{\max}^2}{T_{\min} T} \frac{\varepsilon^2}{12} = \frac{r}{(1-r)^2} \frac{1+c}{1-c} \frac{\varepsilon^2}{12} \qquad (37)$$

with $T_{\max} = \max_{k \in \mathbb{Z}} T_k$, since $\|\mathcal{S}^{-1}\| \le (1-r)^{-1}$ and

$$\mathbb{E}[\epsilon_k \epsilon_m] = \delta_{k,m} \mathbb{E}[\epsilon_k^2] = \delta_{k,m} \int_{-\varepsilon/2}^{\varepsilon/2} \frac{1}{\varepsilon} x^2 dx = \delta_{k,m} \frac{\varepsilon^2}{12} \qquad (38)$$

and, finally

$$\int_{-nT_{\min}}^{nT_{\min}} \sum_{k \in \mathbb{Z}} \sum_{m \in \mathbb{Z}} T_m T_k g(t - s_k) g(t - s_m) dt \cdot \mathbb{E}[\epsilon_k \epsilon_m]$$
$$\le T_{\max}^2 \sum_{k \in \mathbb{Z}} g^2(t - s_k) \frac{\varepsilon^2}{12}.$$

C. Example

A natural comparison between the effects of amplitude and time quantization can be established if we assume that the quantized amplitudes and quantized trigger times are transmitted at the same bitrate. Since $x(s_k)$ and T_k are associated with the trigger times t_k and t_{k+1}, the same transmission bitrate is achieved if $x(s_k)$ and T_k are represented by the same number of bits N. With $-c \le x \le c$, the amplitude quantization step amounts to $\varepsilon = 2c/2^N$.

For time encoding $T_{\min} = \min_{k \in \mathbb{Z}} T_k \le T_k \le \max_{k \in \mathbb{Z}} T_k = T_{\max}$, or equivalently $0 \le T_k - T_{\min} \le T_{\max} - T_{\min}$. Therefore, if $T_{\min}$ is exactly known, then only measuring $T_k - T_{\min}, k \in \mathbb{Z}$, in the range $(0, T_{\max} - T_{\min})$ is needed. Hence

$$\Delta = \frac{T_{\max} - T_{\min}}{2^N} = \frac{1}{2^N} \left(\frac{\delta}{1-c} - \frac{\delta}{1+c} \right) = \frac{\delta \varepsilon}{1 - c^2}.$$

Substituting the values of ε and Δ above into (26) and (36) results exactly in the same upperbound for both the expected MSE for time encoding and irregular sampling, respectively.

Result 1: For the same number of bits N, the upperbound for time quantization is equal to the upperbound for amplitude quantization and amounts to

$$\frac{1}{3 \cdot 2^{2N}} \cdot \frac{r}{(1-r)^2} \cdot \frac{1+c}{1-c} \cdot c^2.$$

Figs. 9 and 10 show the MSE $\mathcal{E}$ in decibels as a function of oversampling ratio σ (see below)) and the number of quantization bits, N, respectively. The details of the simulation are as before. Squares and stars depict the MSE for time encoding
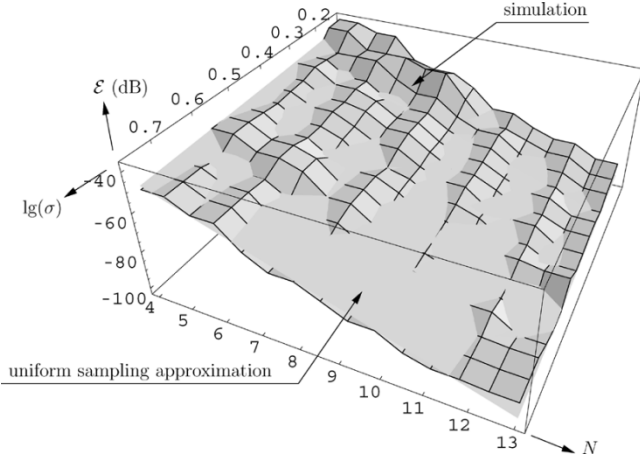
Fig. 11. Dependence of $\mathcal{E}$ in decibels on the number of bits N and the logarithmic oversampling ratio σ and its comparison with the uniform sampling approximation in the time encoding case.

and irregular sampling, respectively. Figs. 9 and 10 also depict the (same) upperbound arising in the inequalities (26) and (36). The dashed traces depict the uniform sampling approximation for $S = (T_{\max} + T_{\min})/2 = \delta/(1 - c^2)$.

Result 2: The MSE of the uniform sampling approximation in decibels depends logarithmically on the oversampling ration σ and linearly on the number of quantization bits N and is given by

$$\mathbb{E}[\mathcal{E}^2]\,[dB] \simeq 10 \cdot \lg\left(\frac{c^2(1-c^2)^2}{3}\right) - 20 \cdot \lg(2)\cdot N - 10\cdot\lg(\sigma).$$

Proof: Let $\sigma = T/S = \pi(1 - c^2)/\Omega\delta$ denote the oversampling ratio. By taking the $10 \cdot \lg$ on both sides of (31) and noting that the integral is approximately equal to 2Ω, the desired result is obtained.

Finally, Fig. 11 depicts the dependance of the MSE $\mathcal{E}$ in decibels on the oversampling ratio σ and the number of quantization bits N. This representation may be used as a practical guide for achieving a target average MSE by means of adjusting the oversampling ratio or the number of quantization bits or both.

VIII. CONCLUSION

Here, we have established time encoding as an alternative information representation modality for bandlimited signals. We have shown that a simple TEM can be used to generate a sequence of trigger times and demonstrated an algorithm that uses this sequence for perfect signal recovery.

We have established a relationship between time encoding and irregular sampling and shown the common structure between time encoding and a number of nonlinear modulation schemes including, FM and Asynchronous sigma-delta Modulation. We have demonstrated how to construct a TDM that only employs the time sequence generated by the TEM. No additional knowledge about the parameters of the TEM is required.

We derived an upperbound on the expected MSE of signal recovery when a quantized version of the trigger times is available. We have also shown that quantization in the time and amplitude domains leads to largely equivalent information repre-

sentations for bandlimited signals. The availability of high precision clocks, however, makes the quantization of the time sequence an alternative to amplitude quantization.

Time encoding is an asynchronous information representation modality. As such, it represents an alternative to the classical clock-based sampling representations. Information of a time encoded bandlimited signal is only contained in its time transitions. In contrast, the information of the output stream of a synchronous sigma–delta modulator resides solely in its amplitude. As such time encoding and synchronous sigma–delta are dual modulation schemes.

The results presented here raise a number of important research questions that, due to space limitations, could not be addressed in this paper. These pertain to the intrinsic performance of the TEM and TDM pair under various conditions arising in practice as well as in comparison with other modulation/demodulation schemes. Boundary effects that are due to the finite signal support, real-time recovery, the effects of noise and parameter variation as well as errors introduced by the evaluation of the pseudoinverse belong to the former. A comparison with synchronous sigma–delta modulation belongs to the latter. We plan to address these and other [13] questions elsewhere.

APPENDIX A
Geometry of Hilbert Spaces

Definition 1: A nonnegative real-valued function $\|\cdot\|$ defined on a vector space E is called a norm if for all $x \in E$

$$\|x\| = 0 \Leftrightarrow x = 0 \tag{39}$$
$$\|x + y\| \leq \|x\| + \|y\| \tag{40}$$
$$\|\alpha x\| = |\alpha|\|x\|. \tag{41}$$

Definition 2: A normed linear space is called complete if every Cauchy sequence in the space converges, that is, for each Cauchy sequence (x_n) there is an element x in the space such that $x_n \to x$.

Definition 3: An inner product on a vector space E over $\mathbb{C}$ (or $\mathbb{R}$), is a complex-valued function $\langle \cdot, \cdot \rangle$ defined on $E \times E$ to $\mathbb{C}$ such that

$$\langle x + y, z \rangle = \langle x, z \rangle + \langle y, z \rangle \tag{42}$$
$$\langle \alpha x, y \rangle = \alpha \langle x, y \rangle \tag{43}$$
$$\langle x, y \rangle = \langle y, x \rangle^* \tag{44}$$
$$\langle x, x \rangle \geq 0, \langle x, x \rangle = 0, \qquad \text{if } f\, x = 0. \tag{45}$$

Definition 4: A complete vector space whose norm is induced by an inner product is called a Hilbert Space.

Example: Let L^2 be the set of functions of finite energy, i.e.,

$$L^2(\mathbb{R}) = \left\{ f \mid \int_{\mathbb{R}} |f(u)|^2 du \langle \infty \right\}$$

with norm $\|f\| = \int_{\mathbb{R}} |f(u)|^2 du$. $L^2(\mathbb{R})$ endowed with the inner product $\langle x, y \rangle = \int_{\mathbb{R}} x(u)y(u)du$ is a Hilbert Space.

There are two important class of operators in a Hilbert space: the projection operators and the adjoint operators.

Definition 5: Operators $\mathcal{B}$ and $\mathcal{B}^*$ defined on Hilbert space $\mathcal{H} \rightarrow \mathcal{H}$ are said to be adjoint if

$$\langle \mathcal{B}x, y \rangle = \langle x, \mathcal{B}^*y \rangle$$

for all $x, y \in \mathcal{H}$.

Definition 6: Let $L^2(\mathbb{R})$ be the Hilbert space of bounded energy functions and let B be the subset of bandlimited functions. The projection operator $\mathcal{P}$ maps an arbitrary function in $x \in L^2$ into a bandlimited function in B through

$$\mathcal{P}x = (g * x)(t)$$

where $*$ denotes the convolution and $g = \sin(\Omega t)/\pi t$.

APPENDIX B
Three Inequalities

Lemma 5 (Bernstein's Inequality): If $f = f(u)$ is a function defined on $\mathbb{R}$ bandlimited to $[-\Omega, \Omega]$ then df/dt is also bandlimited and

$$\left\| \frac{df}{du} \right\| \leq \Omega \|f\|.$$

Proof: By applying Parseval's formula [15], we have

$$\|f'\|^2 = \frac{1}{2\pi} \|(f')\hat{}\|^2 = \frac{1}{2\pi} \|j\omega \hat{f}(\omega)\|^2$$
$$\leq \frac{\Omega^2}{2\pi} \|\hat{f}\|^2 = \Omega^2 \|f\|^2$$

where $\hat{}$ denotes the Fourier transform.

Remark 10: Usually, Bernstein's inequality is stated for the class of bounded bandlimited signals [20], [15] that form a complete vector space with the norm defined as $\|f\| = \sup_{u \in \mathbb{R}} |f(u)|$. The inequality is formally the same.

Lemma 6 (Wirtinger's Inequality): If $f, df/dt \in L^2(a, b)$ and either $f(a) = 0$ or $f(b) = 0$, then

$$\int_a^b |f(u)|^2 du \leq \frac{4}{\pi^2}(b-a)^2 \int_a^b \left| \frac{df}{du} \right|^2 du.$$

Proof: An elementary and highly intuitive proof is based on the observation that

$$\int_0^{\pi/2} \left[\frac{df}{du} - f(u) \cot u \right]^2 du$$
$$= \int_0^{\pi/2} \left(\left| \frac{df}{du} \right|^2 - f^2 \right) du + \int_0^{\pi/2} d(f^2 \cot u)$$

and since

$$\int_0^{\pi/2} d(f^2 \cot u) = 0$$

if $f(0) = 0$ and $df/dt \in L^2(a, b)$, we get

$$\int_0^{\pi/2} \left(\left| \frac{df}{du} \right|^2 - f^2 \right) du \geq 0$$

and the result follows via a change of variables. Motivation for the above proof and generalizations can be found in [6, Sect. 7.7, p. 184].

Proof of Lemma 2: $\mathcal{A}$ and $\mathcal{A}^*$ are adjoint if

$$\langle \mathcal{A}x, y \rangle = \langle x, \mathcal{A}^*y \rangle$$

for any bandlimited functions x and y. Using the linearity properties of the inner product and the fact that $g * x = x$ we have

$$\langle \mathcal{A}x, y \rangle = \left\langle \sum_{k \in \mathbb{Z}} \int_{t_k}^{t_{k+1}} x(u)du\, g(\cdot - s_k), y \right\rangle$$
$$= \sum_{k \in \mathbb{Z}} \int_{t_k}^{t_{k+1}} x(u)du\, y(s_k)$$
$$= \left\langle x, \sum_{k \in \mathbb{Z}} 1_{[t_k, t_{k+1}]} y(s_k) \right\rangle$$
$$= \left\langle g * x, \sum_{k \in \mathbb{Z}} 1_{[t_k, t_{k+1}]} y(s_k) \right\rangle$$
$$= \left\langle x, \sum_{k \in \mathbb{Z}} g * 1_{[t_k, t_{k+1}]} y(s_k) \right\rangle = \langle x, \mathcal{A}^*y \rangle.$$

Proof of Lemma 3: It is easy to see that the adjoint operator $\mathcal{A}^*$ defined in (11) can be written as

$$\mathcal{A}^* = \sum_{\in \mathbb{Z}} x(s_k) \mathcal{P} 1_{[t_k, t_{k+1}]}.$$

Note that

$$\|x - \mathcal{A}^*x\|^2 = \left\| \mathcal{P}x - \sum_{k \in \mathbb{Z}} x(s_k) \mathcal{P} 1_{[t_k, t_{k+1}]} \right\|^2$$
$$\leq \left\| \sum_{k \in \mathbb{Z}} [x - x(s_k)] 1_{[t_k, t_{k+1}(t)]} \right\|^2$$
$$= \sum_{k \in \mathbb{Z}} \int_{t_k}^{t_{k+1}} |x(u) - x(s_k)|^2 du.$$

By applying Wirtinger's inequality, we obtain

$$\int_{t_k}^{t_{k+1}} |x(u) - x(s_k)|^2 du$$
$$= \int_{t_k}^{s_k} |x(u) - x(s_k)|^2 du + \int_{s_k}^{t_{k+1}} |x(u) - x(s_k)|^2 du$$
$$\leq \frac{4}{\pi^2}(s_k - t_k)^2 \int_{t_k}^{s_k} |x'(u)|^2 du$$
$$+ \frac{4}{\pi^2}(t_{k+1} - s_k)^2 \int_{s_k}^{t_{k+1}} |x'(u)|^2 du$$

and, therefore

$$\|x - \mathcal{A}^*x\|^2 \leq \frac{1}{\pi^2} \left(\frac{\delta}{1-c} \right)^2 \sum_{k \in \mathbb{Z}} \int_{t_k}^{t_{k+1}} |x'(u)|^2 du$$
$$\leq \frac{1}{\pi^2} \left(\frac{\delta}{1-c} \right)^2 \|x'\|^2.$$

Finally, by applying Bernstein's inequality we have

$$\|x - \mathcal{A}^* x\| \le r\|x\|.$$

Since $\|\mathcal{A}\| = \|\mathcal{A}^*\|$

$$\|x - \mathcal{A}x\| \le r\|x\|$$

and the lemma follows.

APPENDIX C
Results

Result 3:

$$\frac{1}{2n} \int_{-nT_{\min}}^{nT_{\min}} \sum_{k \in \mathbb{Z}} g^2(t - \hat{s}_k) dt \le \frac{1}{T}$$

and

$$\frac{1}{2n} \int_{-nT_{\max}}^{nT_{\max}} \sum_{k \in \mathbb{Z}} g^2(t - \hat{s}_k) dt \ge \frac{1}{T}$$

and in the limit equality is achieved.

Proof: Increasing the density of packing in the interval $[-nT_{\min}, nT_{\min}]$ implies

$$\int_{-nT_{\min}}^{nT_{\min}} \sum_{k \in \mathbb{Z}} g^2(t - \hat{s}_k) dt$$
$$\le \int_{-nT_{\min}}^{nT_{\min}} \sum_{k \in \mathbb{Z}} g^2\left(t - \frac{T_{\min}}{2} + kT_{\min}\right) dt$$

since the function $g^2(t - \hat{s}_k)$ is positive for all $t, t \in \mathbb{R}$. The infinite sum $\sum_{k \in \mathbb{Z}} g^2(t - T_{\min}/2 - kT_{\min})$ represents a periodic function and

$$\frac{1}{2nT_{\min}} \int_{-nT_{\min}}^{nT_{\min}} \sum_{k \in \mathbb{Z}} g^2\left(t - \frac{T_{\min}}{2} + kT_{\min}\right) dt$$

represents its zeroth-order Fourier coefficient. By applying Parseval's relationship [15], this coefficient amounts to

$$\frac{1}{T_{\min}} \int_{\mathbb{R}} g^2\left(t - \frac{T_{\min}}{2}\right) dt$$
$$= \frac{1}{T_{\min}} \frac{1}{2\pi} \int_{\mathbb{R}} 1_{[-\Omega, \Omega]} d\omega = \frac{1}{T_{\min}} \frac{\Omega}{\pi} = \frac{1}{T_{\min} T}.$$

The second inequality is similarly derived by noting that decreasing the packing in the interval $[-nT_{\max}, nT_{\max}]$ implies

$$\int_{-nT_{\max}}^{nT_{\max}} \sum_{k \in \mathbb{Z}} g^2(t - \hat{s}_k) dt$$
$$\ge \int_{-nT_{\max}}^{nT_{\max}} \sum_{k \in \mathbb{Z}} g^2\left(t - \frac{T_{\max}}{2} + kT_{\max}\right) dt.$$

The rest of the proof is as above.

Result 4:

$$\mathbb{E}[\epsilon_k \epsilon_m] = \left(\frac{\delta}{T_k}\right)^2 \frac{\Delta^2}{12} \delta_{k,m}.$$

Proof: With $d_k = \hat{T}_k - T_k$

$$\epsilon_k = \int_{t_k}^{t_{k+1}} x(u) du - \int_{\hat{t}_k}^{\hat{t}_{k+1}} x(u) du - (-1)^k d_k.$$

Using the mean-value theorem, we obtain

$$\epsilon_k = x(\xi_k) T_k - x(\hat{\xi}_k) \hat{T}_k - (-1)^k d_k$$

where $\xi_k \in (t_k, t_{k+1})$ and $\hat{\xi}_k \in (\hat{t}_k, \hat{t}_{k+1})$. For Δ small enough, $\xi_k \simeq \hat{\xi}_k$ and

$$\epsilon_k \simeq (-x(\xi_k) - (-1)^k) d_k.$$

Since

$$x(\xi_k) = \frac{1}{T_k} \int_{t_k}^{t_{k+1}} x(t) dt = -(-1)^k + (-1)^k \frac{\delta}{T_k}$$

we have

$$\epsilon_k \simeq = -(-1)^k \frac{\delta}{T_k} d_k$$

and thus

$$\mathbb{E}[\epsilon_k \epsilon_m] = (-1)^{k+m} \frac{\delta}{T_k} \frac{\delta}{T_m} \mathbb{E}[d_k d_m] = \left(\frac{\delta}{T_k}\right)^2 \frac{\Delta^2}{12} \delta_{k,m}.$$

Result 5: Assuming that the quantization error $d_k = \hat{T}_k - T_k, k \in \mathbb{Z}$, is a sequence of i.i.d. random variables on $[-\Delta/2, \Delta/2]$, and the t_k's are uniformly spaced

$$\int_{\mathbb{R}} \mathbb{E} e(t) e(t+\tau) e^{-j\omega\tau} d\tau = \frac{\Delta^2}{12} \cdot \frac{\delta^2}{S^3} \cdot \left|\frac{\frac{\omega S}{2}}{\sin\left(\frac{\omega S}{2}\right)}\right|^2 \cdot G(\omega) \quad (46)$$

where $S = t_{k+1} - t_k$ for all $k, k \in \mathbb{Z}$, and G is the Fourier transform of g.

Proof: Let $\hat{c}_k, k \in \mathbb{Z}$, denote the set of coefficients when the quantized trigger times $\hat{t}_k, k \in \mathbb{Z}$, are usedfor recovery. We have

$$\int_{\mathbb{R}} \mathbb{E} e(t) e(t+\tau) e^{-j\omega\tau} d\tau$$
$$= \int_{\mathbb{R}} \sum_{k \in \mathbb{Z}} g\left(t - kS - \frac{S}{2}\right) \sum_{l \in \mathbb{Z}} g\left(t + \tau - lS - \frac{S}{2}\right)$$
$$\times \mathbb{E}[(c_k - \hat{c}_k)(c_l - \hat{c}_l)] e^{-j\omega\tau} d\tau$$
$$= G(\omega) \cdot \left|\frac{\frac{\omega S}{2}}{\sin\left(\frac{\omega S}{2}\right)}\right|^2 \cdot \frac{\Delta^2}{12} \cdot \frac{\delta^2}{S^3}$$

since, by the Poisson formula [15]

$$\sum_{k \in \mathbb{Z}} g\left(t - kS - \frac{S}{2}\right) e^{-j\omega kS}$$
$$= \frac{1}{S} \sum_{k \in \mathbb{Z}} G\left(\omega - k\frac{2\pi}{S}\right) e^{j(\omega - k(2\pi/S))(t - S/2)}$$

and

$$\epsilon_k = \sum_{l \in \mathbb{Z}} \int_{kS}^{(k+1)S} g\left(u - lS - \frac{S}{2}\right) du \cdot (c_l - \hat{c}_l)$$

implies

$$\sum_{l \in \mathbb{Z}} e^{-j\omega(l-k)S} \mathbb{E}[(c_k - \hat{c}_k)(c_l - \hat{c}_l)]$$

$$= \left| \frac{\frac{\omega S}{2}}{\sin\left(\frac{\omega S}{2}\right)} \right|^2 \cdot \frac{\Delta^2}{12} \cdot \frac{\delta^2}{S^2}.$$

REFERENCES

[1] E. D. Adrian, *The Basis of Sensation: The Action of the Sense Organs*. London, U.K.: Christophers, 1928.

[2] E. H. Armstrong, "A method for reducing disturbances in radio signaling by a system of frequency modulation," *Proc. IRE*, vol. 24, no. 5, 1936.

[3] W. R. Benett, "Spectra of quantized signals," *Bell Syst. Tech. J.*, vol. 27, pp. 446–472, 1948.

[4] R. J. Duffin and A. C. Schaeffer, "A class of nonharmonic Fourier series," *Trans. Amer. Math. Soc.*, vol. 72, pp. 341–366, 1952.

[5] H. G. Feichtinger and K. Gröchenig, "Theory and practice of irregular sampling," in *Wavelets: Mathematics and Applications*, J. J. Benedetto and M. W. Frazier, Eds. Boca Raton, FL: CRC Press, 1994, pp. 305–363.

[6] G. H. Hardy, J. E. Littlewood, and G. Pólya, *Inequalities*. New York: Cambridge Univ. Press, 1952.

[7] S. Jaffard, "A density criterion for frames of complex exponentials," *Michigan Math. J.*, vol. 38, no. 3, pp. 339–348, 1991.

[8] C. J. Kikkert and D. J. Miller, "Asynchronous delta sigma modulation," in *Proc. IREE*, vol. 36, Apr. 1975, pp. 83–88.

[9] V. A. Kotel'nikov, "On the transmission capacity of the ether and wire in electrocommunications," in *Modern Sampling Theory, Mathematics and Applications*, J. J. Benedetto and P. J. S. G. Ferreira, Eds. Boston, MA: Birkhauser, 2001, pp. 27–45.

[10] A. A. Lazar and L. T. Toth, "Time encoding and perfect recovery of bandlimited signals," in *Proc. IEEE Int. Conf. Acoustics, Speech, and Signal Processing*, vol. VI, Hong Kong, Apr. 6–10, 2003, pp. 709–712.

[11] ——, "Sensitivity analysis of time encoded bandlimited signals," in *Proc. IEEE Int. Conf. Acoustics, Speech, and Signal Processing*, vol. 2, Montreal, QC, Canada, May 17–21, 2004, pp. 901–904.

[12] A. A. Lazar, "Time encoding with an integrate-and-fire neuron with a refractory period," *Neurocomput.*, vol. 58–60, pp. 53–58, 2004.

[13] A. A. Lazar, E. K. Simonyi, and L. T. Tóth, "Fast recovery algorithms for time encoded bandlimited signals," Dep. Elect. Eng., Columbia Univ., New York, BNET Tech. Rep. #1-04, 2004.

[14] F. Marvasti and M. Sandler, "Applications of nonuniform sampling to nonlinear modulation, A/D and D/A techniques," in *Nonuniform Sampling, Theory and Practice*, F. Marvasti, Ed. New York: Kluwer, 2001, pp. 647–687.

[15] A. Papoulis, *Signal Analysis*. New York: McGraw-Hill, 1977.

[16] E. Roza, "Analog-to-digital conversion via duty-cycle modulation," *IEEE Trans. Circuits Syst. II*, vol. 44, pp. 907–917, Nov. 1997.

[17] A. B. Spirad and D. L. Snyder, "A necessary and sufficient condition for quantization errors to be uniform and white," *IEEE Trans. Acoust., Speech Signal Processing*, vol. ASSP-25, pp. 442–448, Oct. 1977.

[18] C. E. Shannon, "Communications in the presence of noise," *Proc. IRE*, vol. 37, pp. 10–21, Jan. 1949.

[19] T. Strohmer, "Irregular sampling, frames and pseudoinverse," Master's thesis, Dep. Math., Univ. Vienna, , Vienna, Austria, 1993.

[20] R. M. Young, *Introduction to Nonharmonic Fourier Series*. New York: Academic, 1980.

Aurel A. Lazar (S'77–M'80–SM'90–F'93) has been a Professor of Electrical Engineering, Columbia University, New York, NY, since 1988. In the mid 1980s and 1990s, he pioneered investigations into networking games and programmable networks. In addition, he conducted research in broadband networking with quality of service constraints; and in architectures, network management and control of telecommunications networks. His current theoretical research interests are in biological networks; focusing on time encoding and information representation in sensory systems, as well as spike processing and computation in the cortex. His experimental work focuses on resilient networks. More information about his education and research activities can be found at http://ee.columbia.edu/~aurel.

László T. Tóth received the M.S. and Candidate's (Ph.D) degrees from the Technical University, Budapest, Hungary, and the Hungarian Academy of Sciences, Budapest, Hungary, in 1982 and 1987, respectively.

He is an Associate Professor in the Department of Telecommunications and Media Informatics, Budapest University of Technology and Economics, Budapest, Hungary. He worked for the Research Institute for Telecommunications (1982–1993, Budapest, Hungary), Bell Laboratories (1996–1997, Murray Hill, NJ), and Columbia University (1989–1990, 1995–1996, New York, NY). He taught at the Technical University of Budapest (1993–1999) and Columbia University (1999–2002).